A Mossbauer study of electrodeposited $Fe_{1-x}Co_x$ alloys

1993 J. Phys.: Condens. Matter 5 927

(http://iopscience.iop.org/0953-8984/5/7/020)

J. Phys.: Condens. Matter 5 (1993) 927–934. Printed in the UK

A Mössbauer study of electrodeposited $Fe_{1-x}Co_x$ alloys

E Jartych†‡, J K Zurawicz† and M Budzyński‡

† Department of Physics, Technical University of Lublin, ulica Nadbystrzycka 38, 20-618 Lublin, Poland

‡ Institute of Physics, M Curie-Sklodowska University, Place M Curie-Sklodowskiej 1, 20-031 Lublin, Poland

Received 27 July 1992, in final form 15 October 1992

Abstract. The specimens of $Fe_{1-x}Co_x$ alloys obtained by electrodeposition onto graphite were tested by Mössbauer spectroscopy and x-ray diffraction. Two structural transformations from the body-centred cubic to the face-centred cubic and further to the hexagonal, as the Co concentration increases, were observed. How the hyperfine field depends on the occupancies of the 3d and 4s states was deduced. Changes in the preferred direction of domain magnetization caused by the variable Co concentration have also been observed.

1. Introduction

In recent years, many experimental and theoretical studies have been devoted to testing the interesting magnetic properties of alloys and intermetallic compounds of Fe–Co [1–4]. The main objectives were to determine the changes in the hyperfine magnetic field (HMF) and the isomer shift (IS), which occurred in specimens made by melting Fe and Co. The type of magnetic order and the crystalline structure were also determined.

Very recently, alloys prepared by electrodeposition have been used for Mössbauer testing [5–8]. Electrodeposition is a very simple method allowing one to obtain films of high purity and required thickness. It is useful to compare the properties of the Fe–Co alloys obtained by the thermal and electrolytic methods. The purpose of the research described below was to test the crystalline structure and to evaluate the parameters of the hyperfine interactions in the electrodeposited Fe–Co alloys over all the concentration range.

2. Experimental details

Specimens of $Fe_{1-x}Co_x$ alloys were prepared by electrodeposition onto graphite. The electrolyte did not contain the brightness additions commonly used in industry and it consisted of $FeCl_2.4H_2O$ (39.7 g dm^{-3}), $CoCl_2.6H_2O$ (47.6 g dm^{-3}), HCl and H_2O. In order to obtain specimens with various Fe and Co concentrations, the areas of the submerged iron and cobalt anodes were changed. The cathode potential was $U = -2.5$ V for all the specimens. The specimens were deposited at room

0953-8984/93/070927+08$07.50

temperature and a constant pH of 2.7. The current density was between 8.9 and 17.3 mA cm^{-2}; the time of deposition was between 1 and 3.5 h.

The thickness of the deposited films depends on the current density and the time of deposition. The mass of the deposit was measured by weighing the graphite base and the specimen obtained after rinsing and drying. The thickness of the alloys was determined on the basis of the mass, the area of the specimens and the average density of the alloy (the density ρ_{Fe} of iron is 7.86 g cm^{-3}, the density $\rho_{hex\,Co}$ of hexagonal cobalt 8.836 g cm^{-3} and the density $\rho_{cub\,Co}$ of cubic cobalt 8.788 g cm^{-3} [9]). The average thickness of the deposited films was between 3.0 and 21.6 μm.

X-ray diffraction tests were performed using an x-ray diffractometer and the Bragg–Brentano method.

Mössbauer measurements were carried out at room temperature using a standard constant-acceleration spectrometer. The source was ^{57}Co(Cr) of 50 mCi activity.

The alloy composition was determined by the quantitative chemical analysis (atomic absorption spectroscopy). The accuracy of the determination of the composition was as follows: the relative standard deviations for Fe were between 0.5 and 4.5% of the iron contents and for Co were between 0.5 and 3.1% of the cobalt contents in the alloy.

3. Results and discussion

Cobalt and iron constitute solid solutions over all the concentration range. In this experiment, alloys of Co concentrations between 0 and 64 at.% were body centred cubic (BCC), between 65 and 97 at.% face centred cubic (FCC) and over 97 at.% hexagonal close packed (HCP). The lattice parameters of the HCP-structured specimens are given in table 1.

Figure 1 shows the variation in the lattice parameter a with the Co concentration for the BCC and FCC structures. The results of our tests on the BCC Fe–Co alloys ($x < 0.64$) do not conform to the theoretical calculations [10]. In that work it was calculated that the equilibrium lattice constant of the Fe–Co alloys increased with increasing Co concentration, reached a maximum value at about 25 at.% Co and then decreased to the value equal to the lattice constant of pure iron when the Co concentration is about 60 at.%. The results of our experiment show, however, that the lattice parameter of the BCC electrodeposited Fe–Co alloys slightly decreases when the Co concentration increases.

Table 1. Lattice parameters of HCP-structured specimens.

Co concentration (at.%)	a (Å)	c (Å)
99.97	2.5011	4.0886
99.96	2.5036	4.0886
98.50	2.5086	4.1221

All the $Fe_{1-x}Co_x$ alloys are ferromagnetic. The spectral lines are a little broader than those of pure iron. Typical Mössbauer spectra at various Co concentrations are shown in figure 2(*a*). The experimentally obtained spectra were fitted using

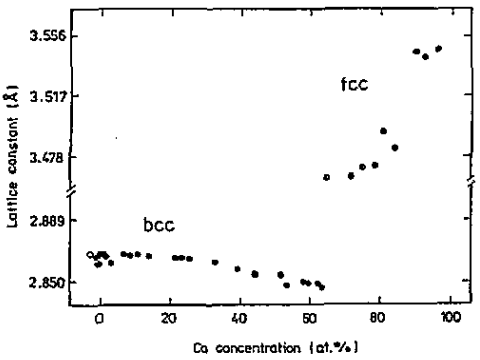

Figure 1. Lattice parameter of Fe–Co alloys as a function of the Co concentration for the BCC and FCC structures: ●, electrodeposited specimens; ○, conventionally prepared sample of pure iron.

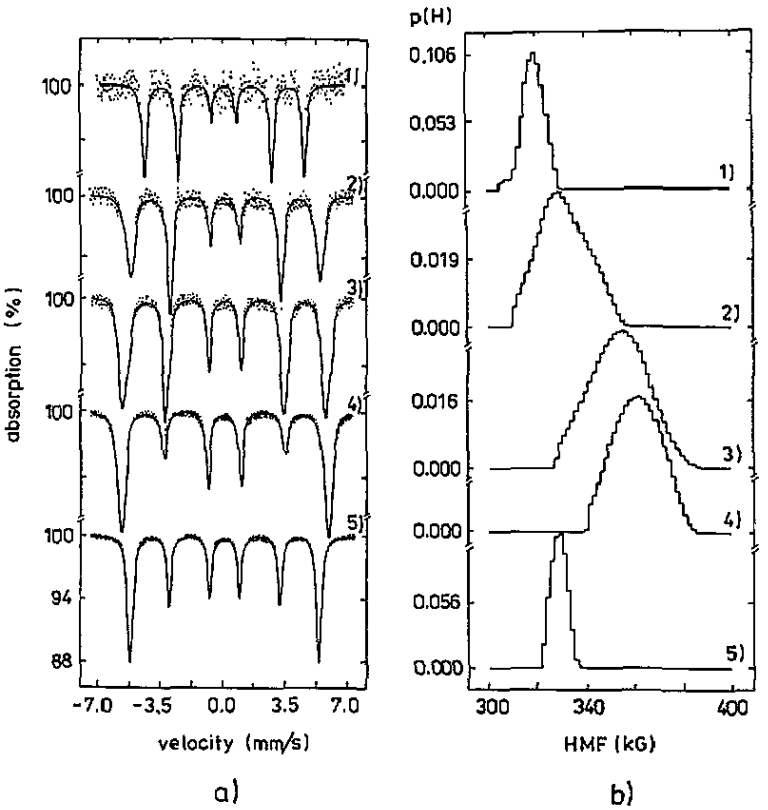

Figure 2. (*a*) Room-temperature Mössbauer spectra and (*b*) HMF distributions for the alloys: curves 1, $Fe_{0.0004}Co_{0.9996}$; curves 2, $Fe_{0.25}Co_{0.75}$; curves 3, $Fe_{0.55}Co_{0.45}$; curves 4, $Fe_{0.77}Co_{0.23}$; curves 5, pure Fe.

the continuous hyperfine field distribution by the Hesse–Rübartsch [11] method. Examples of the field distribution are shown in figure 2(*b*).

Figure 3 shows the average hyperfine field as a function of the Co concentration and as a function of the mean number of electrons per atom. The average hyperfine field at the Fe site shows the maximum which corresponds to the maximum bulk magnetization from the Slater–Pauling curve. No discontinuities have been observed, within the limits of experimental error, during the structural transformations of BCC

to FCC and of FCC to HCP. The observed maximal value of the average field occurs in the alloy containing about 30 at.% Co. This result conforms to the experimental data and the theoretical calculations described in [10].

To compare our results with those obtained for conventionally prepared alloys (by melting) we also show in figure 3 the average HMFs at ^{57}Fe from [12]. There are some differences in the values of the average hyperfine fields, but the general trend is the same. Similar differences in the hyperfine fields were observed for electrodeposited and metallurgical Fe–Ni alloys [13].

No essential differences were observed for the hexagonally structured alloys in the hyperfine field.

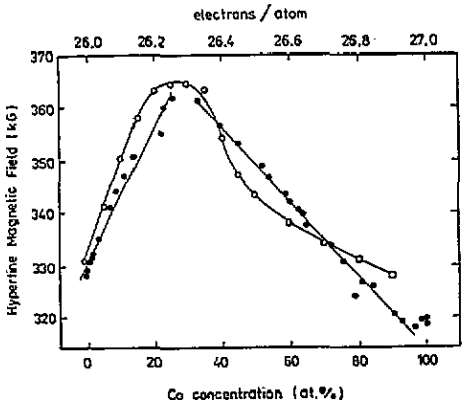

Figure 3. The average HMF as a function of the Co concentration and the mean number of electrons per atom: ●, our experimental data; straight lines, least-squares fit; ○, □, experimental data from [12] for thermally prepared Fe–Co alloys.

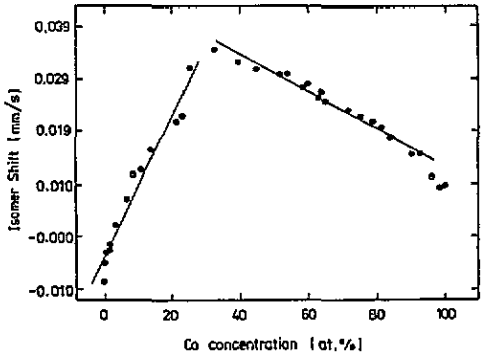

Figure 4. The average IS of ^{57}Fe (relative to pure Fe) as a function of the Co concentration at room temperature.

The IS is proportional to the total density of s electrons in the ^{57}Fe nucleus and depends on the electron structure of the Fe atom and its environment. IS as a function of the Co concentration is shown in figure 4. In accordance with the theoretical calculations by the single-band binding CPA method [3], the number of d electrons in the Fe atoms increases relative to pure iron when the Co concentration in the BCC Fe–Co alloys increases. On the assumption that the density of the 4s electrons does not vary, the increase in the number of 3d electrons causes the number of 3s electrons to decrease, so that the IS becomes larger. In [12] it was established that the IS is positive with respect to pure iron and the electron density at Fe nuclei decreases when iron is alloyed with other metals. In our experiment the IS of electrodeposited $Fe_{1-x}Co_x$ alloys changes its sign relative to the IS of pure iron. Thus for $x < 0.03$ the sign of the IS is negative and for $x > 0.03$ it is positive in relation to that of pure iron (figure 4). There may be a difference between thermally prepared and electrodeposited alloys in the case $x = 0$, i.e. pure iron. In the electrodeposited layers there are interior stresses due to the high concentration of defects [13]. Interior stresses may cause the distances between atoms to decrease and further the pressure to increase. Furthermore, the lattice constant of electrodeposited Fe is a little smaller than the lattice constant of a conventionally prepared sample of pure iron (see figure 1), and this may also be

a reason for the increase in the pressure. On the other hand it is known [14] that for α-Fe the increase in the pressure causes a decrease in the IS. So a negative sign of the IS relative to the IS for pure iron is possible. Moreover our results do not conform to the theoretical calculations [10]. The course of the changes is similar but the theoretically calculated IS values are several lines larger than those measured by us experimentally.

For both Co concentrations $x < 0.30$ and Co concentrations $x > 0.30$ the dependence IS(x) is linear. We can write (as in [4]) that at a given Co concentration the IS depends on x as follows:

$$d(IS)/dx = [\partial(IS)/\partial n_{3d}](dn_{3d}/dx) + [\partial(IS)/\partial n_{4s}](dn_{4s}/dx). \qquad (1)$$

Considering only the BCC- and FCC-structured specimens, the straight-line slope factors were calculated using the least-squares method and the results are as follows: for $x < 0.30$, $d(IS)/dx = +0.128$ mm s^{-1} and for $x > 0.30$, $d(IS)/dx = -0.035$ mm s^{-1}. These results conform approximately to those from [4].

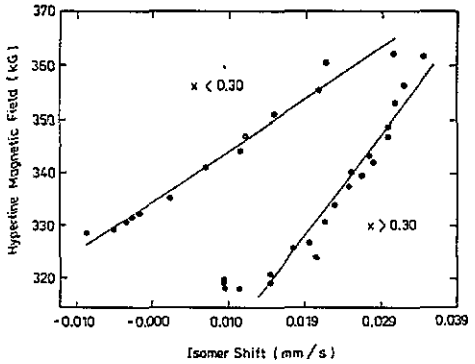

Figure 5. The average HMF as a function of the average IS at room temperature.

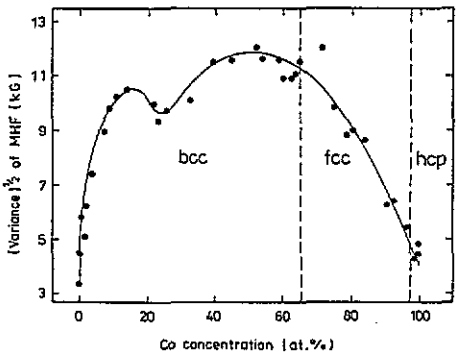

Figure 6. The square root $(\langle H^2\rangle - \langle H\rangle^2)^{1/2}$ of the variance of the ^{57}Fe HMF distribution of electrodeposited Fe–Co alloys as a function of the Co concentration.

The description of the Mössbauer spectra allowed us to obtain the dependence of the average hyperfine field as a function of the IS (figure 5). In our work on the Fe–Ni alloys [15] we have paid attention to the mutual dependence between these two quantities. A similar relation also occurs for the Fe–Co alloys investigated. The statement in [10] that such a relation does not exist is therefore not true.

It should be noted that at both $x < 0.30$ and $x > 0.30$ the function H(IS) is linear. The calculated straight-line slope factors are as follows: for $x < 0.30$, $dH/d(IS) = 979.612$ kG mm^{-1} s and for $x > 0.30$, $dH/d(IS) = 1950.148$ kG mm^{-1} s. The hyperfine field depends on the electron structure of the alloy so that it is connected with the 3d and 4s electron density fluctuations. For a given Co concentration value x, the dependence is as follows:

$$dH/d(IS) = (\partial H/\partial n_{3d})[dn_{3d}/d(IS)] + (\partial H/\partial n_{4s})[dn_{4s}/d(IS)]. \qquad (2)$$

The unknown values $dn_{3d}/d(IS)$ and $dn_{4s}/d(IS)$ were calculated using the quantities $dn_{3d}/dx = +0.72$ electrons for $x < 0.30$, $dn_{3d}/dx = -0.48$ electrons for $x > 0.30$

and $dn_{4s}/dx = -0.02$ electrons based on [4], and from the results of our work: $d(IS)/dx = 0.128$ mm s^{-1} for $x < 0.30$ and $d(IS)/dx = -0.035$ mm s^{-1} for $x > 0.30$. After solving equation (2) for the concentration ranges $x < 0.30$ and $x > 0.30$ the following values resulted: $\partial H/\partial n_{3d} = 162.02$ kG/electron and $\partial H/\partial n_{4s} = -460.19$ kG/electron.

On the basis of figure 3, one can agree that the dependence of the average hyperfine field on x is also linear for appropriate concentration values. The slope factors of the straight lines are equal: for $x < 0.30$, $dH/dx = 128.26$ kG and, for $x > 0.30$, $dH/dx = -71.44$ kG. One can therefore write one more equation:

$$dH/dx = (\partial H/\partial n_{3d})(dn_{3d}/dx) + (\partial H/\partial n_{4s})(dn_{4s}/dx). \tag{3}$$

On the basis of the values of dn_{3d}/dx and dn_{4s}/dx from [4] it was estimated that $\partial H/\partial n_{3d} = 166.42$ kG/electron and $\partial H/\partial n_{4s} = -422.07$ kG/electron. So the average values of the hyperfine field fluctuations caused by the variation in the 3d and 4s electron density are $\partial H/\partial n_{3d} = 164.22$ kG/electron and $\partial H/\partial n_{4s} = -441.13$ kG/electron. The $\partial H/\partial n_{3d}$- and $\partial H/\partial n_{4s}$-values obtained thus are probable, especially the fact that the 3d and 4s electron density fluctuations are small [4]. The signs of $\partial H/\partial n_{3d}$ and $\partial H/\partial n_{4s}$ are different, but it is known [12] that the spin density caused by the 4s electrons in the alloys may be of different signs at various alloy compositions.

Figure 6 shows the square root $(\langle H^2\rangle - \langle H\rangle^2)^{1/2}$ of the variance of the hyperfine field measured on the ^{57}Fe nuclei of electrodeposited Fe–Co alloys. The variance is a measure of the width of the HMF distribution, which reflects the inhomogeneity in local environments of ^{57}Fe nuclei. The measured variance of the HMF distribution for pure iron was not zero; its square root was 3.5 kG. This non-zero value may be connected with some defects in the alloy and with the existence of the grain boundaries in the polycrystalline specimen. The results of our experiment conform well to [4]. Figure 6 also shows the measured HMF variances for the FCC- and HCP-structured alloys.

The average angle θ between the hyperfine field direction and the direction of the absorbed γ-rays may be calculated on the basis of the intensity ratio of the sextet lines [16]:

$$D_{16}/D_{25} = 3(1 + \cos^2\theta)/(4\sin^2\theta) \tag{4a}$$

and

$$D_{25}/D_{34} = (4\sin^2\theta)/(1 + \cos^2\theta) \tag{4b}$$

where D_{16}, D_{25} and D_{34} are the intensities of the lines 1 and 6, 2 and 5, and 3 and 4 in the sextet. From a given angle θ it is possible to calculate the average angle $\phi = 90° - \theta$ between the domain magnetization direction and the plane of the specimen. The results suggest that the magnetization vector has no fixed direction, but it is distributed over an angle range, which means that for $0.00 < x < 0.34$ and $0.90 < x < 0.93$, ϕ belongs to the interval from 43° to 61° and for $0.40 < x < 0.84$ and $0.96 < x < 1.00$, ϕ belongs to the range between 21° and 38°.

4. Conclusions

There are several conclusions that we can draw about the crystalline and magnetic structure of the electrodeposited Fe–Co alloys.

(i) When the concentration of Co dissolved in Fe increases the crystalline structure of the Fe–Co alloy changes from BCC to FCC and further to HCP. In comparison with thermally obtained alloys, the γ-phase appears at a lower Co concentration and the hexagonal structure appears only in alloys of high Co concentration, i.e. over 98 at.%.

(ii) Over the structural transformation ranges there are no discontinuities in the dependence of the hyperfine field on the Co concentration x. This can be interpreted as follows: the interatomic distances d_1 in the FCC and BCC structures are approximately equal, namely $d_1 = 2.4502$ Å for FCC and $d_1 = 2.4648$ Å for BCC, but the number of the nearest neighbours is 12 for FCC and 8 for BCC structures. The different numbers of nearest neighbours may cause the change in the hyperfine field. We suppose that absence of any changes in the hyperfine field was caused by the further neighbours of the ^{57}Fe atom.

(iii) Rather small differences between the values of the hyperfine fields observed for Fe–Co alloys prepared electrolytically and thermally may be connected with the technology. In the electrolytic method, gradual growth of the alloy thickness occurs at room temperature. Therefore differences between the hyperfine interaction parameters for each layer may appear. However, in the thermal method the process of alloy formation usually occurs at a high temperature in the whole volume of the specimen.

(iv) On the simple assumption that at the Co concentrations $x < 0.30$ and $x > 0.30$ the characteristics $H(\text{IS})$ and $H(x)$ are linear, the changes in the hyperfine field caused by the fluctuations in the population of the 3d and 4s levels are equal: $\partial H/\partial n_{3d} = 164.22$ kG/electron and $\partial H/\partial n_{4s} = -441.13$ kG/electron.

Acknowledgments

The authors acknowledge Mr R Dobrowolski and his colleagues from CLAU UMCS for performing the chemical analyses and Mrs M Frak for the diffraction measurements.

References

[1] Vincze I, Campbell I A and Meyer A J 1974 *Solid State Commun.* **15** 1495
[2] Eymery J P, Raju S B and Moine P 1978 *Phys. Lett.* **68A** 260
[3] Hasegawa H and Kanamori J 1972 *J. Phys. Soc. Japan* **33** 1607
[4] Hamdeh H H, Fultz B and Pearson D H 1989 *Phys. Rev.* B **39** 11 233
[5] Kuzmann E, Czako-Nagy I, Vertes A, Chisholm C U, Watson A, El-Sharif M K, Kerti J and Konczos G 1989 *Hyperfine Interact.* **45** 397
[6] Elsukov E P, Vorobev Y N, Trubachev A V and Barinov V A 1990 *Phys. Status Solidi* a **117** 291
[7] Yu Z and Zheng Y 1988 *Hyperfine Interact.* **40** 445
[8] Kovenscky I M and Povetkin V V 1989 *Hyperfine Interact.* **52** 367
[9] 1981 *Search Manual for Selected Powder Diffraction Data for Metals and Alloys* vol 1 (Swarthmore, PA: International Centre for Diffraction Data) pp 119, 542
[10] Akai H 1991 *Hyperfine Interact.* **68** 3
[11] Hesse J and Rübartsch A 1974 *J. Phys. E: Sci. Instrum.* **7** 526

[12] Johnson C E, Ridout M S and Cranshaw T E 1963 *Proc. Phys. Soc.* **81** 1079
[13] Chen R, Yao S, Ge F and Zhou S 1991 *Hyperfine Interact.* **69** 561
[14] Su G, Li F, Xue D, Liu H, Yang Ch and Ge M 1991 *Hyperfine Interact.* **68** 389
[15] Zurawicz J K, Budzyński M and Jartych E 1991 *Proc. 26th Zakopane School on Physics (Singapore, 1991)* ed J Stanek and A T Pedziwiatr (Singapore: World Scientific) p 373
[16] Thosar B V, Srivastava J K, Iyengar P K and Bhargava S C 1983 *Advances in Mössbauer Spectroscopy* (Amsterdam: North-Holland) p 38